Article

Dia-Interacting Protein Modulates Formin-Mediated Actin Assembly at the Cell Cortex

Kathryn M. Eisenmann,[1] Elizabeth S. Harris,[2]
Susan M. Kitchen,[1] Holly A. Holman,[1] Henry N. Higgs,[2]
and Arthur S. Alberts[1,*]
[1] Laboratory of Cell Structure and Signal Integration
Van Andel Research Institute
333 Bostwick Avenue NE
Grand Rapids, Michigan 49503
[2] Department of Biochemistry
Dartmouth Medical School
Hanover, New Hampshire 03755

Summary

Background: Mammalian Diaphanous (mDia)-related formins and the N-WASP-activated Arp2/3 complex initiate the assembly of filamentous actin. Dia-interacting protein (DIP) binds via its amino-terminal SH3 domain to the proline-rich formin homology 1 (FH1) domain of mDia1 and mDia2 and to the N-WASp proline-rich region.
Results: Here, we investigated an interaction between a conserved leucine-rich region (LRR) in DIP and the mDia FH2 domain that nucleates, processively elongates, and bundles actin filaments. DIP binding to mDia2 was regulated by the same Rho-GTPase-controlled autoinhibitory mechanism modulating formin-mediated actin assembly. DIP was previously shown to interact with and stimulate N-WASp-dependent branched filament assembly via Arp2/3. Despite direct binding to both mDia1 and mDia2 FH2 domains, DIP LRR inhibited only mDia2-dependent filament assembly and bundling in vitro. DIP expression interfered with filopodia formation, consistent with a role for mDia2 in assembly of these structures. After filopodia retraction into the cell body, DIP expression induced excessive nonapoptotic membrane blebbing, a physiological process involved in both cytokinesis and amoeboid cell movement. DIP-induced blebbing was dependent on mDia2 but did not require the activities of either mDia1 or Arp2/3.
Conclusions: These observations point to a pivotal role for DIP in the control of nonbranched and branched actin-filament assembly that is mediated by Diaphanous-related formins and activators of Arp2/3, respectively. The ability of DIP to trigger blebbing also suggests a role for mDia2 in the assembly of cortical actin necessary for maintaining plasma-membrane integrity.

Introduction

The Rho family GTPases regulate diverse cellular activities, including actin and microtubule dynamics, gene transcription, cell cycle, and membrane trafficking.

Rho proteins act as binary, nucleotide-dependent switches that promote the formation of distinct actin structures: RhoA, which promotes the formation of stress fibers and focal adhesions; Rac, lamellipodia and membrane ruffles; and Cdc42, filopodia or microspikes [1]. Rho GTPase signaling is achieved by GTP-dependent interactions with autoregulated effector proteins including mammalian Diaphanous-related formins (mDia1, mDia2, and mDia3) and neuronal Wiscott-Aldrich syndrome protein (N-WASp) [2].

mDia protein-mediated actin-filament assembly is controlled by intramolecular interactions mediated by the Dia-inhibitory domain (DID) [3] and Dia-autoregulatory domain (DAD) [4] (Figure 1A). To activate mDia proteins, activated GTPases bind to Armadillo-repeat structures within the GTPase-binding domain (GBD)-DID region and sterically interfere with DAD binding [5, 6]. The release of DAD relieves DID inhibition of the formin homology 2 (FH2) domain, which is then free to nucleate, processively elongate, and (in some cases) bundle nonbranched actin filaments [7, 8]. Whereas mDia proteins assemble actin by direct association with the barbed ends of growing filaments, other GTPase effector proteins, such as those of the WASp/Scar family, indirectly promote actin assembly by stimulating the Arp2/3 complex to bind to preexisting filaments and nucleate branched filaments at their pointed end [2].

The mDia and WASp protein families share several binding partners, including Src, IRSp53, profilin, and Dia-interacting protein (DIP) [9]. DIP is also known as SPIN90, a binding partner for the adaptor Nck. Human DIP is 91% identical to its murine homolog, WISH [10]. Through its amino-terminal SH3 domain, DIP binds to the respective proline-rich regions of N-WASp, mDia1, and mDia2 proteins [10, 11]. Upon binding to N-WASp, DIP stimulates Arp2/3-mediated nucleation independently of Cdc42 [10]; DIP was also shown to bind and directly activate the Arp2/3 complex [12, 13].

Although these studies point to DIP as a positive regulator of N-WASp- and Arp2/3-mediated nucleation of branched filaments, little is known about how DIP influences formin-mediated actin-filament assembly. DIP also bears a polyproline-rich domain (PRD) recognized by the N-WASp and Nck SH3 domains [10, 13] and a conserved C-terminal leucine-rich region (LRR) [11]. The LRR resides within a peptide isolated by a two-hybrid screen with mDia2 as bait [11]. Until now, the LRR interaction with either mDia1 or mDia2 has been uncharacterized.

In this study, we examine the role of the DIP LRR interaction with mDia proteins and identify DIP and the LRR as negative regulators of mDia2-mediated actin-filament assembly. DIP inhibition of mDia2 leads to diminished filopodia assembly and promotes nonapoptotic membrane blebbing, indicating a novel role for formins in the control of actin dynamics at the interface between the cytoskeleton and plasma membrane.
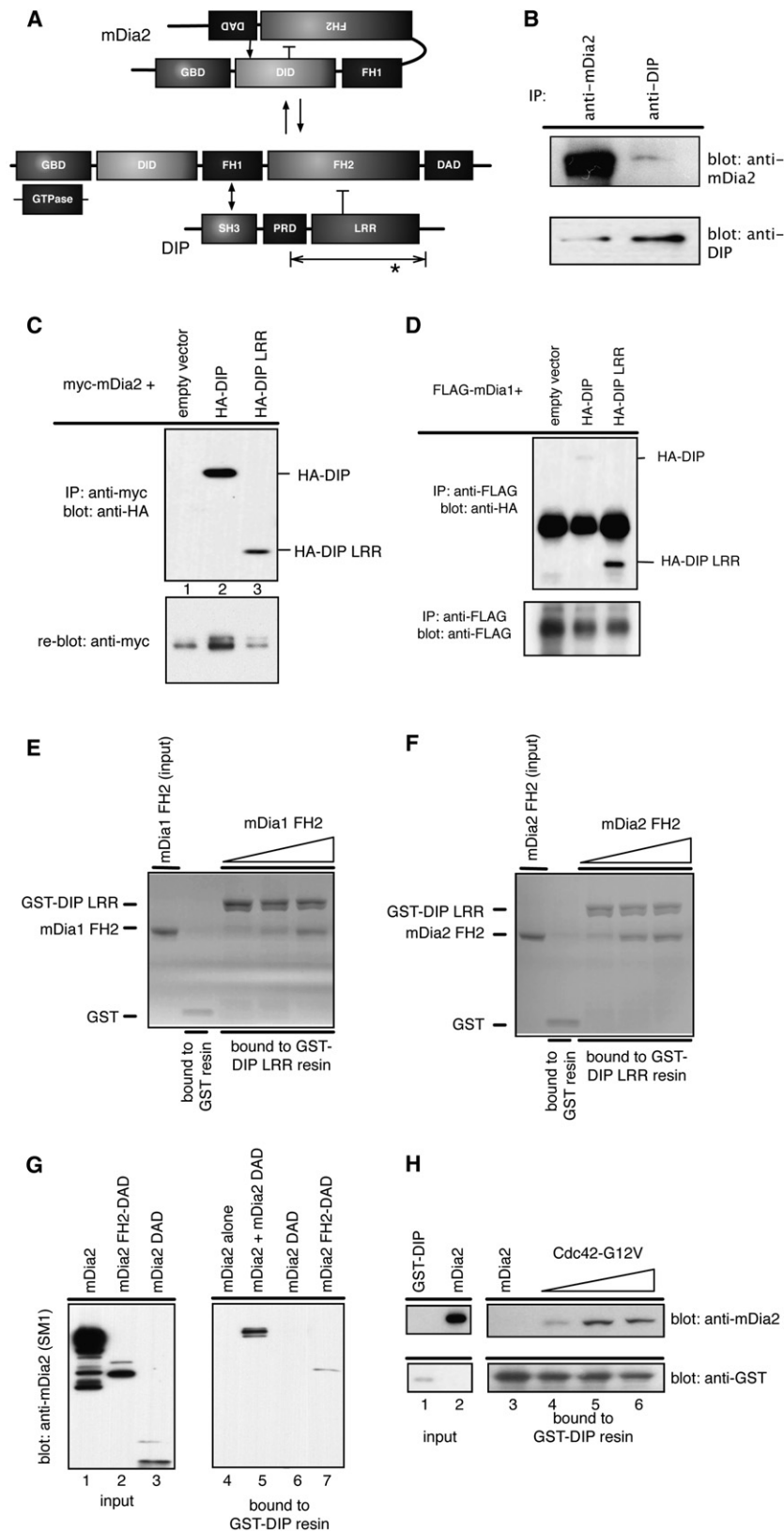
*Correspondence: art.alberts@vai.org

Figure 1. mDia2 Autoregulation Controls the Interaction with DIP

(A) Schematic of Dia-interacting protein and mDia. The line indicated with the asterisk (*) represents the mDia2:DIP interaction originally identified by yeast two-hybrid screen; mDia also interacts with DIP through the mDia2 FH1 and DIP SH3 domains. Abbreviations are as follows: PRD, proline-rich domain; LRR, leucine-rich domain; GBD, GTPase-binding domain; DID, Diaphanous-inhibitory domain; FH1, formin homology domain-1; FH2, formin homology domain-2; and DAD, Dia-autoregulatory domain.

Results

DIP Binds the mDia2 FH2 Region In Vitro and in Cells

The DIP and DIP LRR (Figure 1A) interaction with the mDia2 FH1-FH2 domains was identified previously via two-hybrid screening. The interaction between endogenous DIP and mDia2 was confirmed in HeLa cells by coimmunoprecipitation (Figure 1B). We next confirmed that ectopically expressed mDia and the DIP LRR interact in cells by coimmunoprecipitation. HA-tagged full-length (FL) DIP or DIP LRR was coexpressed in HEK293T cells with epitope-tagged mDia2 or mDia1. FL DIP and DIP LRR were associated with both mDia2 and mDia1 (Figures 1C and 1D, respectively).

The mDia2 FH1 domain also associated with FL DIP (data not shown) but not with DIP LRR, consistent with previous studies [11]. In vitro pulldown assays with a glutathione-S-transferase (GST)-fusion of DIP LRR demonstrated a direct interaction with the purified, recombinant FH2 domains of both mDia1 (Figure 1E) and mDia2 (Figure 1F). This showed that the mDia FH2 domain was sufficient for binding to DIP LRR. The interaction between FL DIP and the isolated FH2 domains was also confirmed (data not shown). Collectively, these data validated DIP's potential for the two following modes of interaction with mDia1 or mDia2: mDia FH1 domains binding to the DIP SH3 domain or mDia FH2 domains interacting with the DIP LRR.

The DIP–mDia2 Interaction Can Be Controlled by Cdc42

To validate a direct interaction between mDia2 and DIP, a GST-fusion of FL DIP was incubated with recombinant FL mDia2, mDia2 FH2-DAD, or mDia2 DAD. In contrast to the immunoprecipitation results (Figures 1B and 1C), FL mDia2 did not bind DIP in vitro (Figure 1G; lane 4). This result led to the hypothesis that DIP binding to the mDia2 FH2 domain was controlled by the autoregulatory mechanism maintained by the mDia DID and DAD domains (Figure 1A) [14].

The mDia autoregulatory mechanism can be unlatched by the addition of DAD peptide [4, 15]. The addition of 0.1 μM DAD induced GST-DIP to bind FL mDia2 (Figure 1G, lane 5). The isolated FH2-DAD region also constitutively bound DIP (lane 7), whereas the DAD alone did not (Figure 1G, lane 6).

mDia2 interacts with multiple Rho GTPases in vitro, including RhoA, Cdc42, and Rif1 [16–18]. Therefore, we tested whether an activated GTPase induced mDia2–DIP binding. Addition of Cdc42 G12V (0.1–0.5 μM) induced a proportionate increase in mDia2 binding to DIP (Figure 1H). Interestingly, GST-DIP LRR binds to FL mDia2 in the absence of GTPase or DAD, suggesting a constitutive association (Figure S1 in the

Supplemental Data available online). Hence, autoregulated mDia2 may be more accessible to DIP LRR than to FL DIP. Indeed, intramolecular interactions between the SH3 and PRD domains may restrict DIP's binding to other proteins, such as mDia or Grb2 [11]. DIP–mDia2 binding represents the first known inducible interaction of the GTPase-regulated formin proteins. Although these observations indicate that the mDia2–DIP interaction is regulated by activated Cdc42, the interaction may also be regulated by other GTPases or mDia- or DIP-binding proteins.

DIP Specifically Inhibits mDia2-Mediated Actin-Filament Assembly

The murine DIP homolog, WISH, binds the nucleation promoting factor N-WASP, and both DIP and WISH directly activate Arp2/3 [12]. We examined the effect of DIP on the ability of mDia2 to assemble actin filaments. As shown previously [7], mDia2 potently accelerates actin polymerization (Figure 2A). Incubating mDia2 with DIP prior to mixing with actin monomers reduced mDia2 nucleation activity in a dose-dependent manner, whereas DIP alone did not alter actin polymerization. Interestingly, mDia1-mediated nucleation was unaffected by incubation with DIP (Figure 2B). Therefore, although DIP binds both mDia1 and mDia2 [11], DIP acts only as a negative regulator of mDia2-mediated actin assembly in vitro.

DIP Disrupts mDia2-Mediated Bundling of Actin Filaments

A subset of formins—including mDia2 and a yeast homolog, Bnr1p—bundle actin filaments, whereas their closely related counterparts mDia1 and Bni1p do not [8, 19]. DIP was tested for an effect on mDia2-mediated filament bundling by low-speed pelleting assays. At low speed, only crosslinked networks of filaments pellet, whereas single filaments remain in the supernatant. The mDia2 FH2 domain caused phalloidin-stabilized actin filaments to pellet in a concentration-dependent manner (Figure 2C). Preincubating mDia2 FH2 domain (400 nM; see Figure 2C, lane 4) with FL DIP reduced the amount of pelleted actin in a concentration-dependent manner (Figure 2D). FL DIP neither pelleted on its own nor caused actin to pellet. Recombinant mDia2 protein containing both the FH1 and FH2 domains was also tested (data not shown); FL DIP inhibited FH1-FH2-mediated bundling, similar to the FH2 domain alone. Thus, DIP acts as a negative regulator of mDia2-associated actin-assembly activities.

DIP Suppression Enhances Filopodia Formation

mDia2 has a role in filopodia assembly [14, 17, 18]. To determine whether DIP affects mDia2 function in cells,

---

(B) HeLa cell lysates were immunoprecipitated and immunoblotted with mDia2 or DIP antibodies.

(C and D) HA-tagged DIP or HA-DIP LRR was coexpressed with Myc-tagged mDia2 (C) or FLAG-tagged mDia1 (D) in HEK293T cells, and anti-Myc (or FLAG) immunoprecipitations were performed. Blots were probed with anti-HA and anti-Myc or FLAG antibodies.

(E and F) In vitro binding assays were performed with 0.4 μM recombinant GST or GST-fused DIP LRR bound to resin and increasing amounts (0.1–10.0 μM) of mDia1 or mDia2 FH2 protein. Recombinant mDia FH2 domain pulled down with GST-DIP LRR was visualized by Coomassie staining.

(G and H) In vitro binding assays were performed with 0.5 μM recombinant GST-fused DIP bound to resin, with 0.1 μM FL mDia2 (aa 1–1171), mDia2 FH2-DAD (aa 609–1171), DAD (aa 1039–1171) or increasing amounts (0.1–0.5 μM) of activated Cdc42 (G12V). Left panels show one-tenth protein input into the assay; right panels show recombinant formin pulled down with GST-DIP resin in the presence or absence of DAD (G) or Cdc42 G12V (H). Proteins were blotted with mDia2 antibodies.
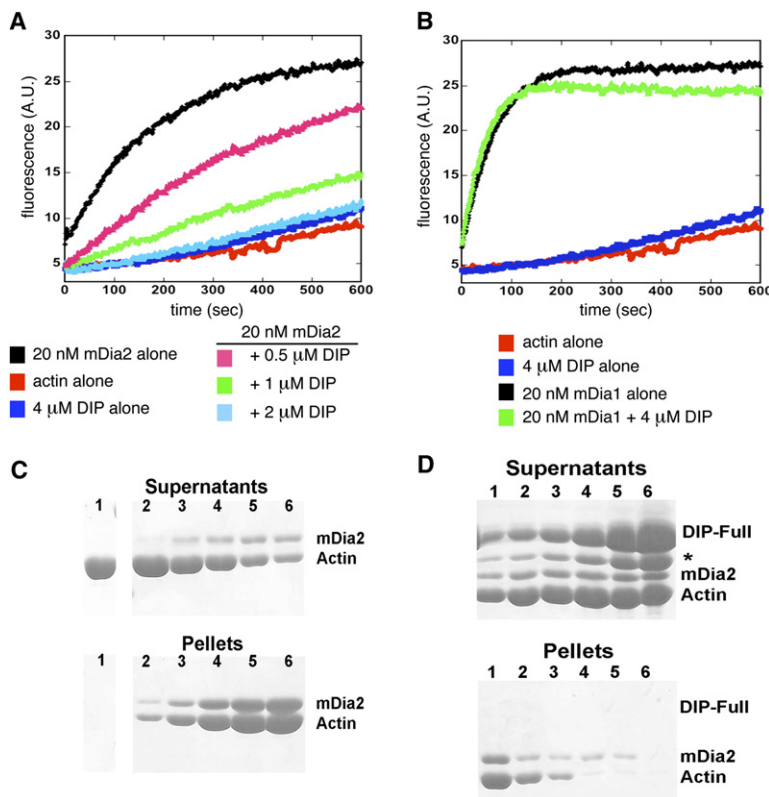
Figure 2. DIP Specifically Inhibits Both mDia2 Actin Nucleation and Filament Bundling

(A and B) Pyrene-actin polymerization assays containing 4 μM monomeric actin and indicated concentrations of formin and DIP constructs. (A) shows 20 nM mDia2 FH2 in the presence of increasing FL DIP. (B) shows 20 nM mDia1 FH2 in the presence of 4 μM DIP. (C and D) Low-speed pelleting assays with 2 μM phalloidin-stabilized actin filaments and mDia2 FH2 domain. Binding and pelleting were conducted in polymerization buffer, and samples separated by SDS-PAGE before staining with Coomassie blue. (C) shows that actin was incubated with increasing concentrations of mDia2. Lanes are described as follows: lane 1, 2 μM actin alone; lanes 2–6, 2 μM actin plus 100, 200, 400, 600, and 800 nM mDia2, respectively. (D) shows that 400 nM mDia2 was incubated with increasing concentrations of DIP-Full. Lanes 1–6 contain 400 nM mDia2 plus 0.25, 0.5, 1, 2, 4, and 8 μM DIP-C (LRR), respectively, plus 2 μM actin. The asterisk marks a breakdown product that could not be purified away from FL DIP.

we suppressed DIP expression by siRNA (Figure S2). HeLa cells expressing DIP siRNA and stimulated with EGF exhibited a striking morphology: Copious filopodia emanated from the cell membrane (Figure 3A and Movie S1). LacZ-siRNA-expressing cells did not differ morphologically from uninjected counterparts (Figure 3A and Movie S1). Fixed DIP-siRNA-expressing cells showed a 50% increase in EGF-induced filopodia when DIP expression was abrogated (Figures 3B and 3C). These data suggest that when DIP is suppressed, mDia2 activity is enhanced.

DIP Interferes with Filopodia Assembly and Triggers Nonapoptotic Membrane Blebbing

We coexpressed DIP with an activator of mDia2 to test whether DIP negatively affects filopodia formation. Cells expressing either CFP-Cdc42-G12V or EGFP-DIP alone or in combination were imaged by time-lapse differential interference contrast (DIC) microscopy to track filopodia formation. Although FL DIP did not affect cell morphology relative to noninjected cells (Figure 4A), activated Cdc42 induced filopodia formation (Figure 4B). In contrast, coexpression of activated Cdc42 with FL DIP caused cells to retract filopodia, round, and then bleb (Figure 4C and Movie S2). Dynamic blebbing occurred in cells coinjected with Cdc42 and DIP in both the presence and absence of EGF (Figure 4C and data not shown). Therefore, DIP not only inhibited filopodia assembly triggered by activated Cdc42 but also affected the machinery that controls membrane integrity.

mDia2 acts as an effector protein for multiple GTPases, including RhoA [9]; RhoA has been shown to localize to blebs [20]. Therefore, cells expressing RhoA

G14V were compared to cells expressing RhoA with FL DIP. Cells expressing CFP-RhoA-G14V were spread out (Figure 4D) with organized stress fibers, consistent with the known effects of activated RhoA. Upon coexpression of RhoA-G14V with FL DIP, cells rounded and blebbed (Figure 4E). The result is consistent with the concept that to bind DIP, mDia2 must be activated by a GTPase (see Figure 1). EGFP-fused DIP LRR expression was sufficient for inducing blebbing (Figure 4F). This result was not surprising given that DIP LRR protein constitutively binds to FL mDia2 in binding assays (data not shown). Purified, recombinant DIP LRR protein microinjected into cells was equally capable of inducing filopodia retraction and blebbing within 10 min (Figure 4F, inset).

Nonapoptotic membrane blebbing is a conserved, physiological process, and it is involved in diverse processes such as cell division, cell spreading, neuronal cell migration, and apoptosis [21–24]. Bleb initiation involves local changes in the contractility of the cortical actinomyosin cytoskeleton by modifying the phosphorylation of myosin II regulatory light chain (MRLC) via myosin light-chain kinase or Rho kinase (ROCK) [25, 26]. Several actin-binding proteins are recruited to blebs in constitutively blebbing cells, including ezrin and moesin [20], indicating that the actin architecture plays a fundamental role in the control of the blebbing mechanism.

Drugs disrupting F-actin or actinomyosin contraction alter blebbing dynamics in constitutively blebbing cell lines [20, 25, 27]. For determining the need for actinomyosin contraction, cells injected with recombinant DIP LRR were treated with blebbistatin, a myosin II

A

siRNA: DIP/EGFP   inset siRNA: DIP   siRNA: lacZ
                                                    EGFP

B

C
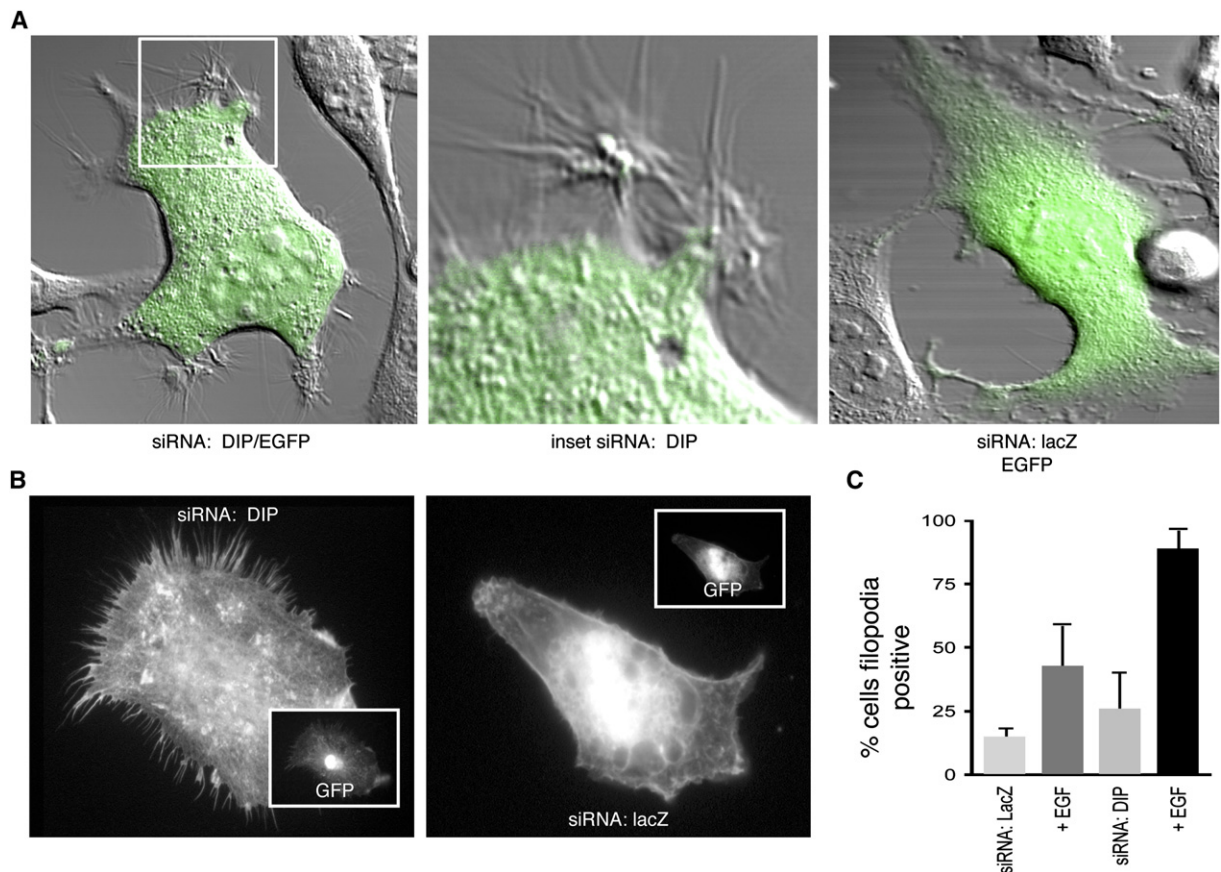
Figure 3. Filopodia Induction upon Diminished DIP Expression

(A) HeLa cells injected with plasmid encoding both EGFP and siRNA against human DIP or lacZ. After 24 hr, cells were stimulated with 2 μM EGF and imaged by live-cell confocal microscopy.

(B) HeLa cells were injected with plasmid encoding both EGFP and siRNA against human DIP or lacZ. After 24 hr, cells were stimulated with 2 μM EGF, fixed after 5 min, and stained with phalloidin. Insets depict EGFP expression in injected cells.

(C) Quantitation of filopodia where 20–40 injected cells were visualized by time-lapse microscopy and scored for blebbing from three independent experiments; error bars represent the mean ± sample SD.

ATPase inhibitor. HeLa cells injected with 0.1 μM DIP LRR protein were imaged for 30 min (Figures S3A and S3C and Movie S3). Cells were then treated with 10 μM blebbistatin and imaged for an additional 30 min. Blebbistatin blocked DIP-LRR-induced blebbing (Figures S3B and S3D and Movie S3), while DMSO-treated cells continued to bleb (Figure S3E). Similar results were obtained with a Rho-kinase inhibitor, Y-27632 (data not shown), indicating that DIP-LRR-mediated blebbing involves Rho kinase-controlled myosin II-dependent contractility.

We next assessed whether DIP expression induces RhoA activation and phosphorylation of MRLC through ROCK I. HEK293T cells were transfected with GFP-fused DIP or DIP LRR, and cell lysates were subjected to pulldown assays with the GST-Rhotekin Rho-binding domain (RBD) and immunoblotted for RhoA. Neither FL DIP nor DIP LRR activated RhoA when compared with control GFP-transfected lysates (Figure S3G). Furthermore, whereas activated ROCK I Opa G1114 enhanced MRLC phosphorylation relative to controls, MRLC phosphorylation was unchanged in FL DIP- or DIP-LRR-transfected cells. These data show that DIP is not a global activator of MRLC phosphorylation and is

therefore not inducing blebbing indirectly through ROCK. However, actomyosin contraction is required for DIP-induced blebbing because both blebbistatin and the Rho-kinase inhibitor (Y-27632) reversibly inhibit blebbing in DIP-LRR-injected cells (Figure S3 and data not shown).

mDia2-Binding-Deficient Variants of DIP LRR Have Impaired Blebbing Activity

Primary amino acid sequence alignments revealed that the DIP LRR is highly conserved (Figure 5A); DIP homologs were identified in budding and fission yeast, insects, and amphibia through database searches. The alignments were used for identifying residues within the LRR potentially mediating the DIP–mDia2 interaction. Several conserved residues (indicated by arrowheads in Figure 5A) were converted to alanine, and plasmids expressing the DIP LRR variants as CFP fusion proteins were cotransfected into HEK293T cells with mDia2; then, coimmunoprecipitations were performed. Although the N555 residue was not perfectly conserved, DIP LRR N555A binding to mDia2 was impaired, and the double-aspartate-substituted D628/634A variant had no appreciable binding defect (Figure 5B).
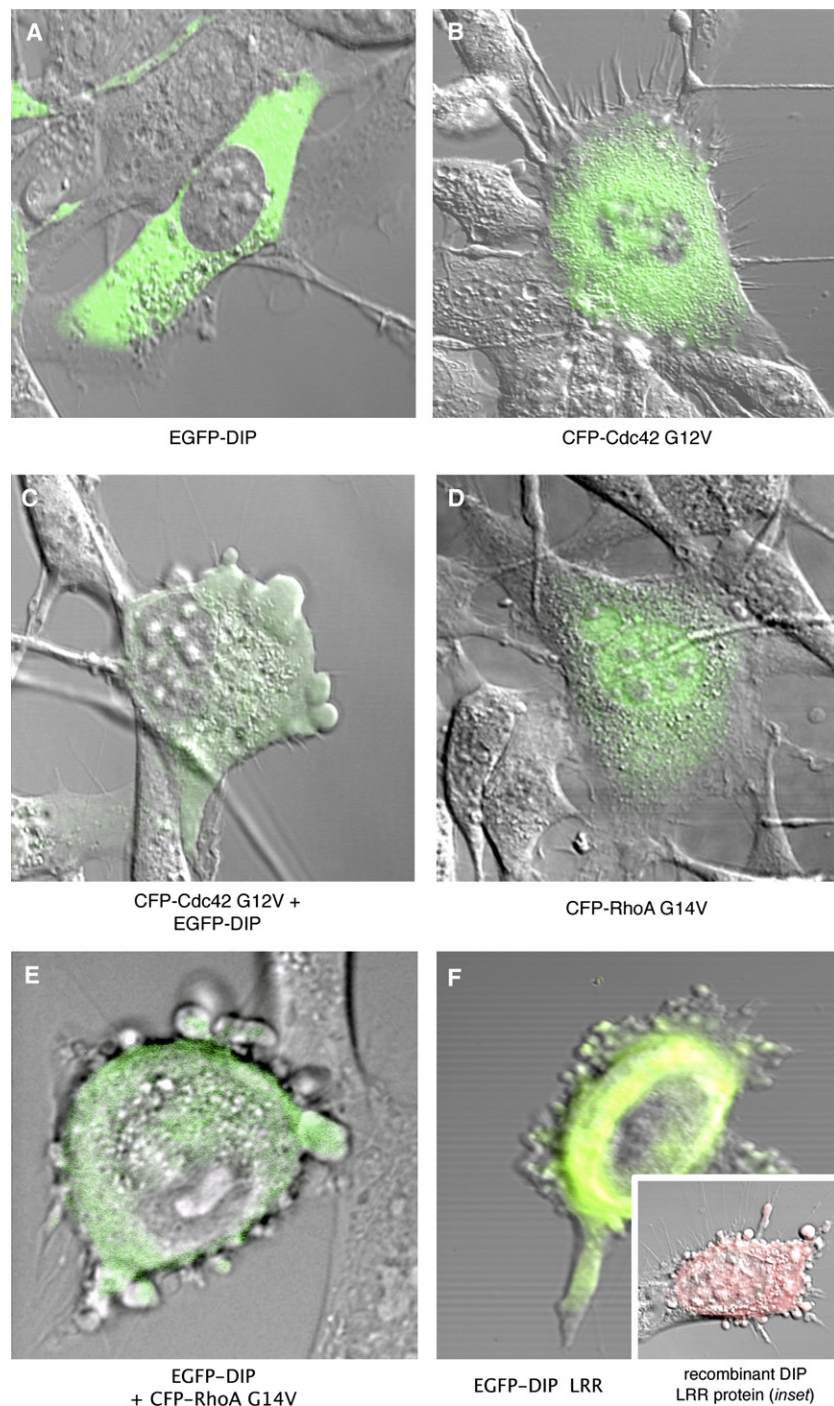
Figure 4. DIP Induces Nonapoptotic Membrane Blebbing

(A–F) HeLa cells were injected with plasmids encoding CFP-Cdc42 G12V, CFP-RhoA G14V (false-colored green) along with EGFP DIP or EGFP DIP LRR as indicated. Four hours after injection, cells were stimulated with 2 μM EGF for 5 min, and live-cell confocal imaging was performed for 10–20 min. The inset of (F) shows HeLa cells injected with 0.1 μM recombinant DIP LRR protein.

The N555A and D628/634A variants were purified as recombinant proteins (Figure 5D and data not shown) and tested in GST pulldowns for mDia2 binding (Figure 5C). Consistent with the coimmunoprecipitation, the N555A DIP variant bound poorly to the FH1-FH2 region of mDia2, whereas D628/634A LRR binding was comparable to the binding of intact DIP LRR. Quantification of DIP LRR N555A binding to the mDia2 FH2 domain showed that binding was compromised when compared with DIP LRR (Figure 5E). The DIP LRR or N555A recombinant proteins (0.1 μM each) were then microinjected into HeLa cells; DIP LRR induced blebbing within 5–20 min (Figure 5F), but N555A LRR induced blebbing in fewer cells. Collectively, these studies indicated that DIP-induced blebbing depends upon its ability to bind to the mDia2 FH2 domain.
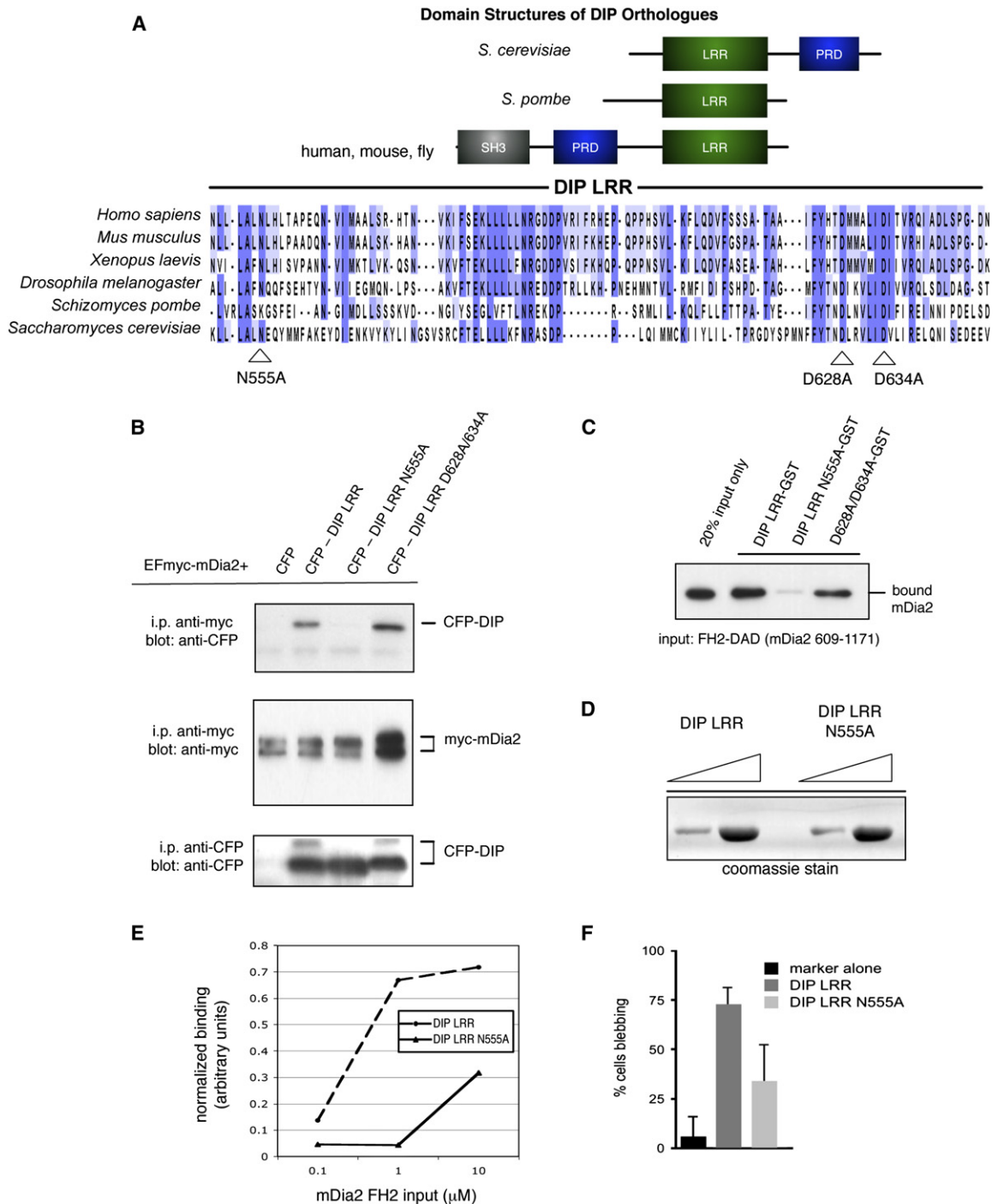
Figure 5. DIP LRR N555A Mutation Perturbs Both Binding to mDia2 and Membrane Blebbing

(A) Schematics illustrating the DIP leucine-rich region across diverse species. Sequence alignments were generated by clustalW analysis; gaps are shown in white. Residues matching the consensus sequence are shown in dark blue. A nonconsensus residue with a positive Blosum62 score is shown in light blue. Arrows indicate residues targeted for alanine substitution. Genbank accession numbers for DIP and its homologs are as follows: *H. sapiens* DIP, BAB63205; *M. musculus* WISH, AAF36503; *X. laevis*, AAH73218; *D. melanogaster*, NP_996372; *S. pombe*, SPBC24C6; and *S. cerevisiae* Ldb17p, YDL146W.

(B) CFP-tagged wild-type or alanine-substituted DIP LRR were coexpressed with Myc-tagged mDia2 in HEK293 cells, and anti-Myc immunoprecipitations were performed. Blots were probed with CFP and Myc antibodies.

(C and D) In vitro binding assays were performed with 0.4 μM recombinant GST-fused wild-type or alanine-substituted DIP LRR bound to resin (shown in [D]), with 0.1 μM mDia2 FH2-DAD. Proteins were blotted with mDia2 antibodies.

(E) In vitro binding assays were performed with 0.4 μM recombinant GST, GST-fused DIP LRR, or DIP LRR N555A bound to resin with 0.1–10.0 μM mDia2 FH2 protein. Recombinant mDia2 FH2 domain pulled down with GST-DIP LRR were visualized by Coomassie staining and quantitated by densitometry.

(F) HeLa cells were injected with recombinant either DIP LRR wild-type or LRR N555A protein and fluorescent dextran, with imaging performed for 10–20 min. Error bars represent the mean percentage of cells blebbing ± the SD.

DIP-Induced Blebbing Is Independent of mDia1 and Arp2/3

DIP-mediated blebbing could be due to effects on mDia1, which binds DIP through its FH1 domain [11]. Alternatively, DIP could directly activate Arp2/3 or inappropriately activate Arp2/3 through N-WASp [10, 12, 13, 28]. Initially, we tested whether mDia1 was required for DIP-induced blebbing. DIP LRR and N555A LRR recombinant proteins were microinjected in 2D6 cells [17]. These mDia1 knockout cells express elevated mDia2 and generate many filopodia. Microinjected cells were fixed and stained with fluorescent phalloidin for visualization of the F-actin architecture (Figure 6A). Relative to cells injected with marker alone (data not shown) or N555A LRR, DIP-LRR-injected cells immediately lost their microspikes (Figure 6B). Within 10–20 min, cells began to bleb (Figure 6C). Therefore, although DIP binds to mDia1, it does not require this interaction to drive membrane blebbing.

Recently, Arp 2/3 was demonstrated to bind the DIP LRR [12]. To address whether the Arp2/3 complex [29] is involved in DIP-mediated blebbing, we injected mouse embryonic fibroblasts (MEFs) expressing siRNA targeting the Arp3 subunit [30] with recombinant DIP or DIP LRR (Figure 7; Movie S4). Despite Arp3 depletion, cells injected with DIP LRR blebbed profusely (Figure 7A), unlike those injected with marker alone (Figure 7B). MEFs expressing control siRNA blebbed upon introduction of DIP LRR (Figure 7C). Furthermore, the numbers of blebbing cells after injection were nearly identical in Arp3 knockdown and control parental MEFs (Figure 7D). Collectively, these data suggest that DIP-mediated bleb induction occurred independently of N-WASp/Arp2/3. This result is consistent with observations made in Arp2/3-defective strains of *Dictyostelium*, which bleb in response to chemoattractant despite the disruption of Arp2/3-mediated actin polymerization [31].

Requirement of mDia2 in DIP-Mediated Blebbing

The assembly of the actin cortex is necessary for dynamic membrane blebbing and requires actin polymerization. However, the identity of the actin nucleator(s) critical for perpetuating the blebbing phenotype remains elusive; not Arp2/3, VASP, or mDia1 localize to blebs or are required for blebbing [20]. We assessed the requirement for mDia2 in DIP-mediated blebbing. siRNA directed against human mDia2 was stably expressed in HeLa cells (Figure S4). mDia2 knockdown cells ruffled extensively (Figure 8B). Control cells injected with recombinant DIP LRR protein rounded and blebbed (Figure 8A; 21/26 cells), whereas mDia2 knockdown cells microinjected with recombinant DIP LRR protein failed to bleb (Figure 8C; 0/21 cells). NIH 3T3 cells, which have little or no detectable mDia2 [11], were also refractory to the effect of microinjected with DIP LRR (Figure 8D; 2/28 cells). However, NIH 3T3 cells expressing a truncated, constitutively active variant of Rho-kinase I (ROCK I-G1114 Opa [25]) (Figure 8E; 23/25 cells) blebbed profusely, indicating that the blebbing machinery downstream of RhoA/ROCK is intact. Finally, HeLa cells expressing dominant-negative mDia (mDia FH2ΔN) blebbed profusely (Figure 8F; 17/23 cells).

Collectively, these data indicate that DIP-induced blebbing depends on mDia2 function.

Discussion

In this study, we uncovered DIP as a negative regulator of mDia2. DIP specifically inhibited mDia2-mediated actin nucleation and bundling activity in vitro, despite its ability to bind both mDia1 and mDia2. DIP disrupted the ability of mDia2 to assemble filopodia and induced exaggerated nonapoptotic membrane blebbing in cells. This phenomenon points to a role for mDia2 in the assembly of F-actin at the cell cortex, which contributes to plasma-membrane morphology. The interaction between DIP and mDia2 is tightly controlled by the mDia2 autoregulatory mechanism that also governs formin-mediated actin nucleation and filament elongation. Thus, DIP-mediated inhibition of mDia2 provides an additional regulatory mechanism complementing the GTPase-controlled intramolecular DID-DAD switch [3].

DIP Binds and Inhibits mDia2-Mediated Actin Nucleation and Filament Bundling

Our results demonstrate that DIP binds to mDia proteins through multiple protein–protein interaction domains. The formin FH1 and FH2 domains bind to the DIP SH3 and leucine-rich C terminus, respectively. Although the binding results are consistent with previously published results [11], in our hands the FL DIP interaction with mDia2 is more robust than the association with mDia1 in cells. The dissimilarities may be significant and warrant further investigation. mDia1 and mDia2 FH2 domains' structural differences, which allow the latter to bind and bundle actin filaments, may account for the differences in sensitivity to DIP. The in vitro experiments, however, do not take into account possible posttranslational modifications, of either binding partner, that may affect the mDia–DIP interaction within cells.

We demonstrate that the DIP–mDia2 interaction is tightly controlled by the GTPase-governed autoinhibitory mechanism. mDia2 autoinhibition can be relieved via introduction of DAD or activated Cdc42, which triggers binding to DIP. Consistent with this model, expression of DIP with either activated Cdc42 or activated RhoA interfered with filopodia assembled by mDia2, but expression of FL DIP had no discernable effect. Together, the data suggest that DIP inhibition of mDia2 depends on the formin first becoming activated. In other words, DIP binding to the FH2 domain is permissive, and the interaction is sequential.

DIP's failure to affect mDia1 also raises the question of what purpose the interaction serves in cells. One possibility is that DIP brings mDia1 and its filament nucleation and elongation activities into proximity with N-WASp or activated Arp2/3 for facilitating cooperation between the machineries driving branched and nonbranched filament assembly [32]. Thus, DIP may act as a pivot between branched and nonbranched actin networks. Likewise, production of dendritic networks would benefit from mDia2 inhibition, which tends to drive filopodia assembly [17, 18]; juxtaposition of mDia1 with the nucleation-promoting factor WASp in cells would
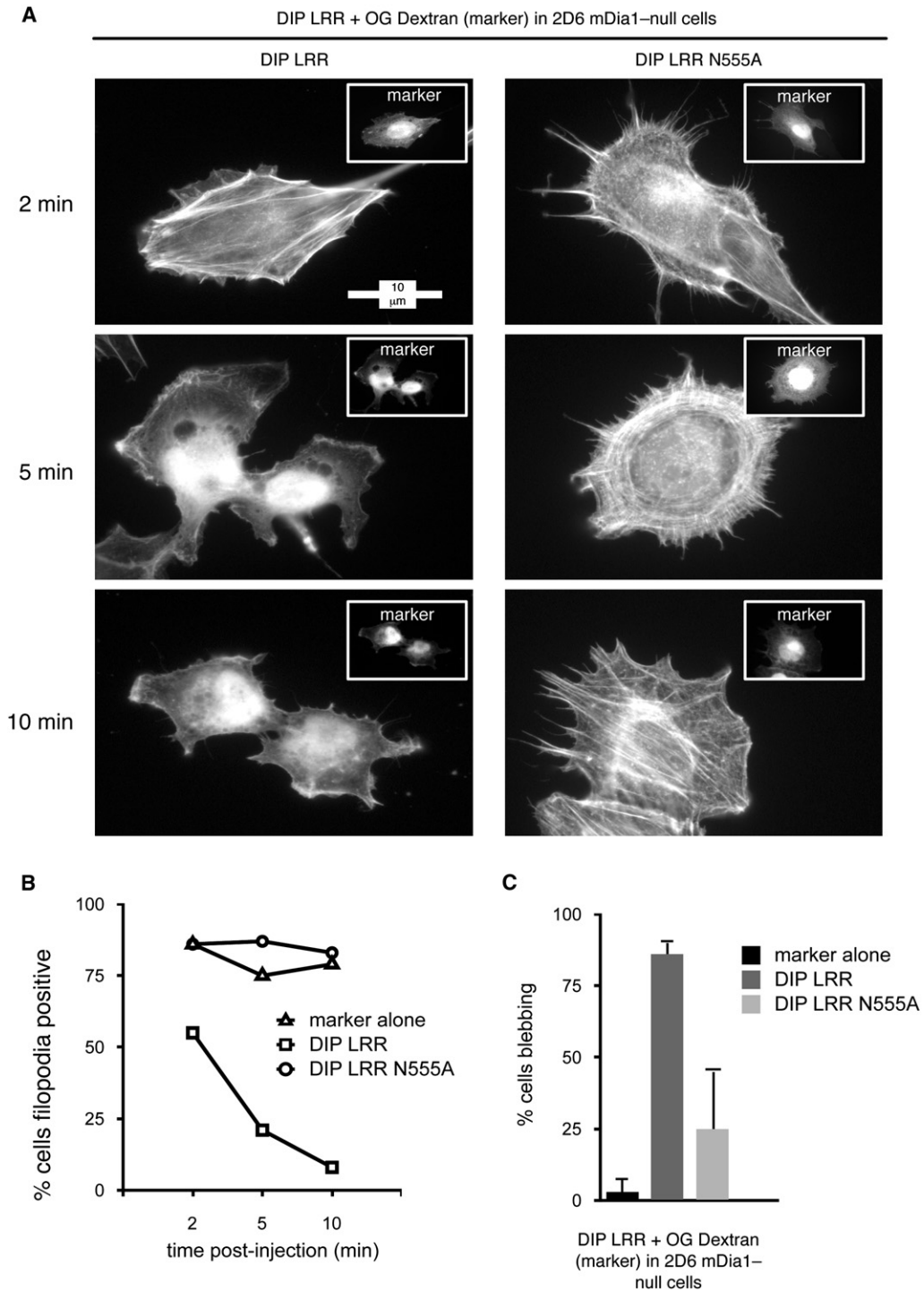
Figure 6. mDia1 Is Not Required for DIP-Mediated Loss of Filopodia nor Membrane Blebbing

(A) 2D6 cells were injected with 0.1 μM purified, recombinant DIP LRR or DIP LRR N555A and Oregon green dextran. Cells were stimulated with 2 μM EGF for 5 min, and cells imaged through 10 min. Cells were fixed at indicated time points and stained with fluorescent phalloidin.
(B) Cells displaying filopodia (filopodia positive); error bars represent the percentage of injected cells with filopodia ± the SEM. Filopodia were quantitated from cells documented in (A) at indicated time points.
(C) Blebbing cells were quantitated from cells documented in (A). Error bars represent the percentage of cells blebbing ± the SD.

allow activated Arp2/3 to utilize newly "minted" filaments nucleated by the formin for side branching [33]. In support of this model, T cells isolated from mDia1 knockout mice fail to ruffle in response to adhesion to stimulatory substrates (K.M.E., unpublished data).

DIP and mDia2 in Cortical Actin-Cytoskeleton Assembly

Dynamic blebbing involves multiple events at the plasma membrane; blebbing is indicative of the integrity of the cell cortex and is an effective readout of cortical
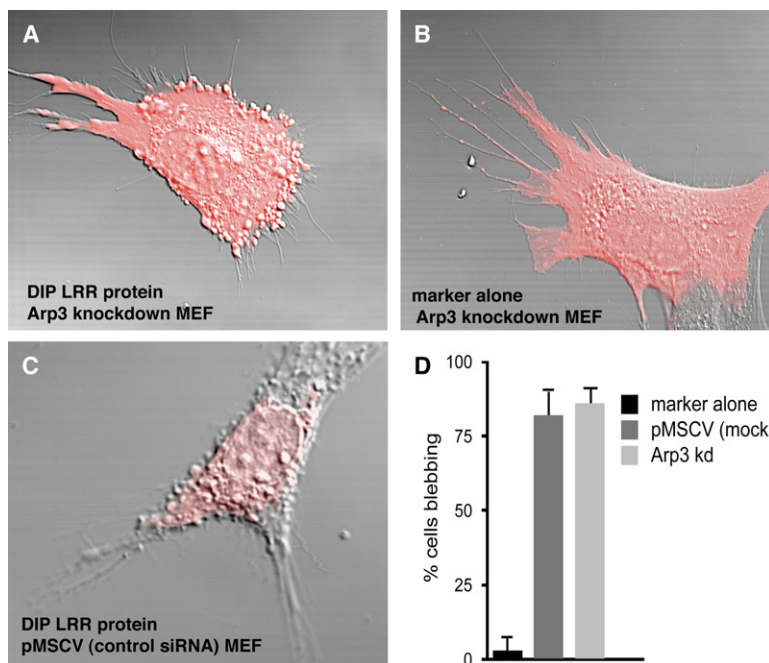
Figure 7. DIP-Mediated Membrane Blebbing Does Not Require Arp2/3

(A–C) MEFs expressing siRNA directed against Arp3 (A and B) or control siRNA (C) were injected with 0.1 μM recombinant DIP LRR or DIP LRR N555A along with Texas-red-dextran marker or marker alone; injected cells were imaged for 10 min by live-cell confocal microscopy.

(D) Blebbing cells were quantitated from cells (A–C); bars represent the mean percentage of blebbing cells ± SD.

tension [34]. Paluch and colleagues [35] postulated that breaks in the actin cortex allow cytoplasm, driven by hydrostatic pressure generated by actomyosin contraction, to exude blebs. Actin polymerization directed into the bleb then participates in retraction of all or part of the bleb. Aspects of this model have been demonstrated in live cells by the visualization of F-actin assembly into nascent blebs [20, 27]. F-actin is localized to the base of expanded blebs, yet not within the bleb itself. Here, we propose a role for mDia2 in maintaining the cortical actin cytoskeleton. We postulate that mDia2 mediates the elongation of F-actin into blebs and failure caused by DIP LRR or DIP overexpression favors the exaggerated bleb formation observed. This suggests an analogous role for mDia2 in blebbing and maintaining the cell actomyosin cortex to that described in the assembly of F-actin within filopodia [14, 17].

A role for formins in bleb retraction was suggested, yet mDia1 failed to localize to the bleb [20]. RhoA is localized within the retracting bleb [16] and may activate mDia2 and promote actin-filament elongation necessary for bleb retraction. Yet, the interaction between DIP and the mDia2 FH2 domain inhibits filament elongation. This paradox may be explained in that the DIP–mDia2 interaction is tightly regulated by the GTPase-dependent autoregulatory mechanism. When deregulated mDia2 interacts with DIP, bleb retraction may be disrupted because of inhibition of filament elongation (visualized through exaggerated blebs). Presumably, all cellular mDia2 does not interact with DIP and thus activated mDia2 not bound to DIP could nucleate and elongate filaments that mediate bleb retraction. Furthermore, it is unknown whether the DIP–mDia2 interaction is reversible or how it is regulated (e.g., by phosphorylation or cellular localization). The regulation of this interaction requires further investigation.

Our results point to a role for mDia2 in maintenance of the cortical actin cytoskeleton; DIP affects this activity in a negative way, leading to blebbing. Knockdown or simple nonexpression of mDia2 is not sufficient for inducing blebbing. One potential explanation is that DIP bound to mDia2 forms a complex that is more than simply inactive; it is also possible the DIP LRR-mDia2 complex *gains* an "interfering" function that allows it to negatively affect existing F-actin structures and induce or exaggerate blebbing. DIP may also affect the activities of its other binding partners. In addition to mDia2, the DIP LRR interacts with a host of other proteins including mDia1, FHOD (weak interaction) [36], and Arp2/3 [12]. Neither mDia1 nor Arp 2/3 localizes to the bleb [20], nor does the loss of their expression affect DIP-LRR-mediated blebbing. Therefore, in the absence of mDia2, DIP LRR might interact with one or more of these proteins and maintain the cortex. DIP may act as a bridge between multiple types of actin nucleators and thus integrate multiple GTPase (in)dependent signaling pathways that affect actin remodeling.

We show that the DIP blebbing mechanism requires myosin contractility, presumably through localized ROCK I-mediated MRLC phosphorylation. However, DIP (or DIP LRR) overexpression enhanced neither global RhoA activation nor MRLC phosphorylation, despite the recent localization of RhoA in the bleb membrane [20]. Blebs induced via DIP are dynamic, suggesting that local changes in the membrane proximal environment (e.g., actin polymerization or bundling) and RhoA activation and MRLC phosphorylation are likely to mediate such changes [37]. Recently, Charras et al. demonstrated localized effects of myosin-II-inhibiting drugs on constitutively blebbing cells, and this suggests that the actomyosin cortex acts locally to promote blebbing [27]. Experiments exploring this hypothesis are currently underway.

Other Roles for DIP in Signaling to the Cytoskeleton
The introduction of DIP LRR both decreased stress-fiber formation and induced blebbing, which potentially enhances cell motility. Indeed, suppression of DIP
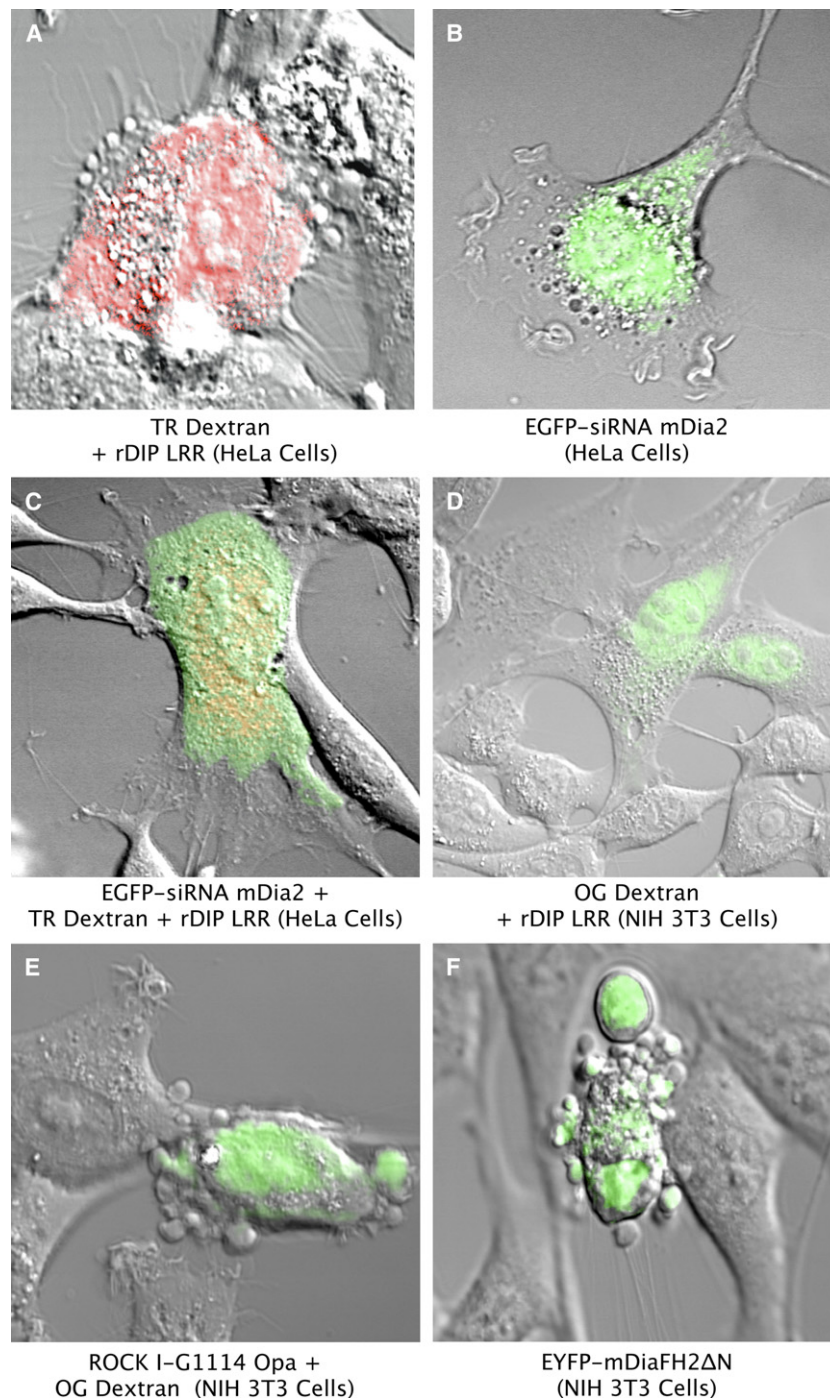
Figure 8. DIP-Mediated Membrane Blebbing Requires mDia2

(A–C) HeLa cells were injected with plasmids encoding both EGFP and siRNA against mDia2 (B and C). At 24 hr, cells were (re)injected with 0.1 μM recombinant DIP LRR and Texas-red (TR)-dextran marker, and cells were imaged by confocal microscopy.

(D and E) NIH 3T3 cells were injected with recombinant DIP LRR (D) or plasmid encoding ROCK I (G1114 Opa) with fluorescent Oregon green (OG) dextran and imaged by confocal microscopy either immediately (D) or 4 hr (E) after injection.

(F) HeLa cells were injected with an EYFP-fused mDia FH2ΔN and imaged by confocal microscopy 4 hr after injection.

expression [38] inhibits directed cell migration, suggesting that DIP functions in cell motility. Therefore, a role for DIP-mediated blebbing may be ascribed for promoting amoeboid-like cancer-cell migration, such as that proposed by Sahai and Marshall [26]. Together, these combined activities for DIP point to a physiological role in cell movement, which in some cases is dependent upon blebbing. Blebbing was associated with motility in fast-moving amoeboid cells [39]. Melanoma cells were shown to oscillate between a bleb and an actin nucleation and polymerization mode (via RhoA and ROCK signaling) to facilitate cell motility [26]. Hence, blebbing

induction via DIP may ultimately promote cancer-cell metastasis.

Experimental Procedures

Cell Culture, Microinjection, Transfection, and Time-Lapse Image Acquisition

HEK293T and HeLa cells were maintained in DMEM containing 10% (v/v) FBS. 2D6 mDia1 null cells were derived as described [17] and were maintained in DMEM containing 10% (v/v) FBS. Arp3 knock-down (kd) and control pMSCV-expressing MEFs [30] (a kind gift from Dr. David J. Kwiatkowski) were maintained in DMEM containing 10% (v/v) FBS, 10 mM HEPES, 1 mM MEM nonessential amino acids, 100 units/ml penicillin, and 100 μg/ml streptomycin.

Cell lines for microinjection were changed to medium containing 0.1% (v/v) FBS 24 hr prior to all microinjections. HeLa and 2D6 cells were plated on glass coverslips as described [17]. HeLa, 2D6, and Arp3 knockdown MEFs were plated onto glass-bottom dishes (Mat-Tek) and incubated for 14 hr in 0.1% DMEM for live-cell time-lapse imaging or immunofluorescence. Cell microinjection and immunofluorescence were performed as previously described [17, 40]. Purified protein was coinjected with Oregon green or Texas red dextran (1 μg/ml) for identifying injected cells.

Time-lapse imaging was acquired with a Zeiss Axiovert 100M (63× objective) fitted with an environmental chamber that maintained cells at 37°C and in a 10% CO$_2$-containing atmosphere. Images were acquired at 10 s intervals with a Zeiss Axiocam controlled by the Improvision software. Live-cell confocal imaging was performed with a Zeiss LSM 510 META confocal laser-scanning microscope with a 25 mW krypton-argon (488, 514, and 568 nm) and HeNe (633 nm) and a Ti-sapphire pulse laser. An environmental chamber maintained cells at 37°C and in a 10% CO$_2$-containing atmosphere. A 0.5 μm slice was acquired at 5 s intervals for 20 min.

Transfection of HEK293T or HeLa cells was performed with Lipofectamine 2000 (Invitrogen) according to the manufacturer's specifications. Cell lysates were prepared in lysis buffer (20 mM Tris-HCl [pH 7.5], 100 mM NaCl, 1% NP40, and 10% glycerol) containing 0.1 M sodium vanadate, 0.1 M aprotinin, 0.1 M pepstatin, 0.1 M leupeptin, 0.1 M dithiothreitol, and 0.1 M PMSF, and immunoprecipitations were performed as described [40].

Recombinant Proteins, In Vitro Binding Assays and Pyrene-Actin-Nucleation Assay

Recombinant proteins were prepared and purified as described by Li and Higgs [15]. Binding assays were carried out by incubation of 0.1 μM mDia2 (aa 1–1171), 0.1 μM mDia2 FH2-DAD (aa 609–1171), 0.1 μM DAD (aa 1039–1171) or 0.1, 0.25, or 0.5 μM Cdc42 G12V with 0.5 μM DIP-GST fusion bound to glutathione beads in TNM buffer (25 nM Tris [pH 7.2], 100 mM NaCl, and 10 mM MgCl$_2$) plus protease inhibitors (1 mM PMSF and 1 mM DTT) for 5 hr at 4°C. Beads were washed thrice in TMN buffer adjusted with 0.1% NP40 and NaCl to 0.15 M.

Pyrene actin nucleation and actin-bundling assays were performed exactly as described by Li and Higgs [15]; recombinant mDia1 and mDia2 FH2 domains with FL DIP proteins were used.

Intracellular Flow Cytometry

Cells (2 × 10^5) were fixed with Fix and Perm Cell Permeabilization Kit (Caltag Laboratories) according to the manufacturer's protocol. Fluorescence was detected with a FACSCalibur flow cytometer (Becton Dickenson).

Rho-Pulldown Assays

The Rhotekin Rho-binding domain was from Upstate (Millipore), and the assay performed according to the manufacturer's specifications. RBD bead loading was assessed by staining of the membrane with Ponceau S (Sigma). Western blots were performed with RhoA antibodies (Santa Cruz).

Antibodies and Plasmids

HA and Myc monoclonal antibodies were from VARI Monoclonal Antibody Core Facility. Myc polyclonal antibodies were from Santa Cruz Biotechnology. GFP/YFP/CFP antibody was from AbCam. DIP rabbit polyclonal antibodies were generated against a C-terminal peptide of murine DIP (aa 587–608). GST antibodies were from Cell Signaling. FLAG antibody was from Chemicon. Texas red phalloidin and Oregon green and Texas red dextran were from Molecular Probes.

EFm (Myc-tagged) mDia2, FLAG-tagged mDia1, and EGFP mDia1 FH1 domain were previously described [4, 40]. DIP FL and DIP LRR were as described [11] and subcloned into pECFP vectors (Clontech) [17]. DIP siRNA sequences were as previously published [38]. mDia2 siRNA sequences were kindly provided by Dr. Shingo Yasuda. Oligos were subcloned into pSuppressor Neo-GFP siRNA vectors (a kind gift from Matt VanBrocklin).

Supplemental Data

Supplemental Data include four figures and four movies and are available with this article online at http://www.current-biology.com/cgi/content/full/17/7/579/DC1/.

References

1. Jaffe, A.B., and Hall, A. (2005). Rho GTPases: Biochemistry and biology. Annu. Rev. Cell Dev. Biol. 21, 247–269.

2. Nicholson-Dykstra, S., Higgs, H.N., and Harris, E.S. (2005). Actin dynamics: Growth from dendritic branches. Curr. Biol. 15, R346–R357.

3. Higgs, H.N. (2005). Formin proteins: A domain-based approach. Trends Biochem. Sci. 30, 342–353.

4. Alberts, A.S. (2001). Identification of a carboxyl-terminal diaphanous-related formin homology protein autoregulatory domain. J. Biol. Chem. 276, 2824–2830.

5. Rose, R., Weyand, M., Lammers, M., Ishizaki, T., Ahmadian, M.R., and Wittinghofer, A. (2005). Structural and mechanistic insights into the interaction between Rho and mammalian Dia. Nature 435, 513–518.

6. Nezami, A.G., Poy, F., and Eck, M.J. (2006). Structure of the autoinhibitory switch in formin mDia1. Structure 14, 257–263.

7. Harris, E.S., Rouiller, I., Hanein, D., and Higgs, H.N. (2006). Mechanistic differences in actin bundling activity of two mammalian formins, FRL1 and mDia2. J. Biol. Chem. 281, 14383–14392.

8. Kovar, D.R., Harris, E.S., Mahaffy, R., Higgs, H.N., and Pollard, T.D. (2006). Control of the assembly of ATP- and ADP-actin by formins and profilin. Cell 124, 423–435.

9. Wallar, B.J., and Alberts, A.S. (2003). The formins: Active scaffolds that remodel the cytoskeleton. Trends Cell Biol. 13, 435–446.

10. Fukuoka, M., Suetsugu, S., Miki, H., Fukami, K., Endo, T., and Takenawa, T. (2001). A novel neural wiskott-aldrich syndrome protein (n-wasp) binding protein, wish, induces arp2/3 complex activation independent of cdc42. J. Cell Biol. 152, 471–482.

11. Satoh, S., and Tominaga, T. (2001). mDia-interacting protein acts downstream of Rho-mDia and modifies Src activation and stress fiber formation. J. Biol. Chem. 276, 39290–39294.

12. Kim, D.J., Kim, S.H., Lim, C.S., Choi, K.Y., Park, C.S., Sung, B.H., Yeo, M.G., Chang, S., Kim, J.K., and Song, W.K. (2006).

Interaction of SPIN90 with the Arp2/3 complex mediates lamellipodia and actin comet tail formation. J. Biol. Chem. *281*, 617–625.

13. Lim, C.S., Kim, S.H., Jung, J.G., Kim, J.K., and Song, W.K. (2003). Regulation of SPIN90 phosphorylation and interaction with Nck by ERK and cell adhesion. J. Biol. Chem. *278*, 52116–52123.

14. Wallar, B.J., Stropich, B.N., Schoenherr, J.A., Holman, H.A., Kitchen, S.M., and Alberts, A.S. (2006). The basic region of the Diaphanous-Autoregulatory Domain (DAD) is required for autoregulatory interactions with the Diaphanous-related formin inhibitory domain. J. Biol. Chem. *281*, 4300–4307.

15. Li, F., and Higgs, H.N. (2005). Dissecting requirements for autoinhibition of actin nucleation by the formin, mDia1. J. Biol. Chem. *280*, 6986–6992.

16. Alberts, A.S., Bouquin, N., Johnston, L.H., and Treisman, R. (1998). Analysis of RhoA-binding proteins reveals an interaction domain conserved in heterotrimeric G protein beta subunits and the yeast response regulator protein Skn7. J. Biol. Chem. *273*, 8616–8622.

17. Peng, J., Wallar, B.J., Flanders, A., Swiatek, P.J., and Alberts, A.S. (2003). Disruption of the Diaphanous-related formin *Drf1* gene encoding mDia1 reveals a role for Drf3 as an effector for Cdc42. Curr. Biol. *13*, 534–545.

18. Pellegrin, S., and Mellor, H. (2005). The Rho family GTPase Rif induces filopodia through mDia2. Curr. Biol. *15*, 129–133.

19. Moseley, J.B., and Goode, B.L. (2005). Differential activities and regulation of Saccharomyces cerevisiae formin proteins Bni1 and Bnr1 by Bud6. J. Biol. Chem. *280*, 28023–28033.

20. Charras, G.T., Hu, C.K., Coughlin, M., and Mitchison, T.J. (2006). Reassembly of contractile actin cortex in cell blebs. J. Cell Biol. *175*, 477–490.

21. Dean, S.O., Rogers, S.L., Stuurman, N., Vale, R.D., and Spudich, J.A. (2005). Distinct pathways control recruitment and maintenance of myosin II at the cleavage furrow during cytokinesis. Proc. Natl. Acad. Sci. USA *102*, 13473–13478.

22. Fishkind, D.J., Cao, L.G., and Wang, Y.L. (1991). Microinjection of the catalytic fragment of myosin light chain kinase into dividing cells: Effects on mitosis and cytokinesis. J. Cell Biol. *114*, 967–975.

23. Trinkaus, J.P. (1973). Surface activity and locomotion of Fundulus deep cells during blastula and gastrula stages. Dev. Biol. *30*, 69–103.

24. Trinkaus, J.P. (1980). Formation of protrusions of the cell surface during tissue cell movement. Prog. Clin. Biol. Res. *41*, 887–906.

25. Coleman, M.L., Sahai, E.A., Yeo, M., Bosch, M., Dewar, A., and Olson, M.F. (2001). Membrane blebbing during apoptosis results from caspase-mediated activation of ROCK I. Nat. Cell Biol. *3*, 339–345.

26. Sahai, E., and Marshall, C.J. (2003). Differing modes of tumour cell invasion have distinct requirements for Rho/ROCK signalling and extracellular proteolysis. Nat. Cell Biol. *5*, 711–719.

27. Charras, G.T., Yarrow, J.C., Horton, M.A., Mahadevan, L., and Mitchison, T.J. (2005). Non-equilibration of hydrostatic pressure in blebbing cells. Nature *435*, 365–369.

28. Lim, C.S., Park, E.S., Kim, D.J., Song, Y.H., Eom, S.H., Chun, J.S., Kim, J.H., Kim, J.K., Park, D., and Song, W.K. (2001). SPIN90 (SH3 protein interacting with Nck, 90 kDa), an adaptor protein that is developmentally regulated during cardiac myocyte differentiation. J. Biol. Chem. *276*, 12871–12878.

29. Pollard, T.D., Blanchoin, L., and Mullins, R.D. (2000). Molecular mechanisms controlling actin filament dynamics in nonmuscle cells. Annu. Rev. Biophys. Biomol. Struct. *29*, 545–576.

30. Di Nardo, A., Cicchetti, G., Falet, H., Hartwig, J.H., Stossel, T.P., and Kwiatkowski, D.J. (2005). Arp2/3 complex-deficient mouse fibroblasts are viable and have normal leading-edge actin structure and function. Proc. Natl. Acad. Sci. USA *102*, 16263–16268.

31. Langridge, P.D., and Kay, R.R. (2006). Blebbing of Dictyostelium cells in response to chemoattractant. Exp. Cell Res. *312*, 2009–2017.

32. Eisenmann, K.M., Peng, J., Wallar, B.J., and Alberts, A.S. (2005). Rho GTPase-formin pairs in cytoskeletal remodelling. Novartis Found. Symp. *269*, 206–218.

33. Bailly, M., Ichetovkin, I., Grant, W., Zebda, N., Machesky, L.M., Segall, J.E., and Condeelis, J. (2001). The F-actin side binding activity of the Arp2/3 complex is essential for actin nucleation and lamellipod extension. Curr. Biol. *11*, 620–625.

34. Paluch, E., Sykes, C., Prost, J., and Bornens, M. (2006). Dynamic modes of the cortical actomyosin gel during cell locomotion and division. Trends Cell Biol. *16*, 5–10.

35. Paluch, E., Piel, M., Prost, J., Bornens, M., and Sykes, C. (2005). Cortical actomyosin breakage triggers shape oscillations in cells and cell fragments. Biophys. J. *89*, 724–733.

36. Westendorf, J.J., and Koka, S. (2004). Identification of FHOD1-binding proteins and mechanisms of FHOD1-regulated actin dynamics. J. Cell. Biochem. *92*, 29–41.

37. Mammoto, A., Huang, S., Moore, K., Oh, P., and Ingber, D.E. (2004). Role of RhoA, mDia, and ROCK in cell shape-dependent control of the Skp2-p27kip1 pathway and the G1/S transition. J. Biol. Chem. *279*, 26323–26330.

38. Meng, W., Numazaki, M., Takeuchi, K., Uchibori, Y., Ando-Akatsuka, Y., Tominaga, M., and Tominaga, T. (2004). DIP (mDia interacting protein) is a key molecule regulating Rho and Rac in a Src-dependent manner. EMBO J. *23*, 760–771.

39. Yoshida, K., and Soldati, T. (2006). Dissection of amoeboid movement into two mechanically distinct modes. J. Cell Sci. *119*, 3833–3844.

40. Tominaga, T., Sahai, E., Chardin, P., McCormick, F., Courtneidge, S.A., and Alberts, A.S. (2000). Diaphanous-related formins bridge Rho GTPase and Src tyrosine kinase signaling. Mol. Cell *5*, 13–25.